

2019

Nanoengineered condenser surfaces for enhancing transport in thermal desalination by air gap membrane distillation

Yashwant S. Yogi

Sina Nejati

Akshay K. Rao

Rishav Roy

Longnan Li

See next page for additional authors

Follow this and additional works at: <https://docs.lib.purdue.edu/mepubs>

This document has been made available through Purdue e-Pubs, a service of the Purdue University Libraries.
Please contact epubs@purdue.edu for additional information.

Authors

Yashwant S. Yogi, Sina Nejati, Akshay K. Rao, Rishav Roy, Longnan Li, Soumyadip Sett, Abhimanyu Das, Nenad Miljkovic, Justin A. Weibel, and David M. Warsinger

Authors and Affiliation:

Yashwant S. Yogi¹, Sina Nejati¹, Akshay K. Rao¹, Rishav Roy¹, Longnan Li², Soumyadip Sett², Abhimanyu Das¹, Nenad Miljkovic², Justin A. Weibel¹, David Warsinger¹.

¹School of Mechanical Engineering, and Birck Nanotechnology Center, Purdue University, West Lafayette

²Department of Mechanical Science and Engineering, University of Illinois, Urbana-Champaign

Presentation Title: “Nanoengineered condenser surfaces for enhancing transport in thermal desalination by air gap membrane distillation”

Track (c) Micro/Nano Scale Phenomena and Thermo-Physical Properties

Topic (c-1) Transport Phenomena in Nano and Molecular Scale Systems

ABSTRACT

Thermal desalination is a technique that uses heat or thermal energy to desalinate water, unlike reverse osmosis. Membrane distillation (MD) is a type of thermal desalination technology having various configurations. Air gap membrane distillation (AGMD) is one of the more energy efficient MD configurations, being especially advantageous over other configurations at high salinity. However, the large mass transfer resistance of the air gap dramatically reduces the permeate flux, impairing performance. Higher condensation performance can be achieved by using a smaller air gap size, but typical film-wise condensation flow patterns flood the air gap at the optimal gap size (<1 mm). Experiments show that dropwise and jumping-droplet condensation regimes, achieved using hydrophobic and superhydrophobic condensing surfaces respectively, can improve droplet shedding, allowing for thinner gap sizes. A system-level numerical model is used to demonstrate that these surfaces could thereby enable improved energy efficiency (2.1× increase of gained output ratio) while avoiding flooding at gap sizes as small as 0.2 mm. Superhydrophobic surfaces with directional jumping of droplets, specifically in the direction of gravity, are also tested and compared to droplets that jump normal to the condensing surface. Novel condensing surfaces that include a combination of the superhydrophobic and superhydrophilic patterns create flow regimes having pathways for faster permeate removal. Other condensing surfaces, including SLIPS (slippery liquid-infused porous surfaces) and laser-ablated superhydrophobic patterned surfaces are tested to check the extent to which they improve the permeate removal rate while exhibiting different condensation regimes that merit further exploration.

KEYWORDS: desalination; membranes; transport; condensation; membrane distillation

1. INTRODUCTION

Membrane distillation (MD) is a thermal desalination technology that uses membranes to distill the salty feed water. Unlike other types of desalination, the driving force is the vapor pressure difference across the membrane instead of externally applied mechanical pressure. This vapor pressure difference across the membrane is the result of the temperature gradient between the feed side and the permeate side of the system. The membranes are hydrophobic in nature and only allow vapor to pass through, making MD systems particularly efficient for handling a high-salinity feed. Once the vapor passes through the membrane, it is condensed and collected on the other side [1,2, 3]. The temperature throughout the system

(operated near atmospheric pressure) is lower than the boiling point of water and generally the feed water is at 60-90°C, which can be easily attained using waste heat and other low-temperature sources like solar heaters [3]. If the temperature of heat source is above 100°C, increasing system pressure to prevent boiling is considered but not preferred due to economic factors and scale formation[4]. At present, the system energy efficiency of MD is less compared to reverse osmosis (RO) systems because it involves phase change [5]. But the use of low-grade waste heat can yield a comparable and sometimes lower cost of operation for MD compared to RO [2,3,6,7]. Membrane distillation is compatible with higher concentrations than normal RO and therefore can be used to concentrate the brine left out from the RO process to help reach close to the saturation concentration. [1,8].

Air gap membrane distillation (AGMD) is one of the leading MD configurations owing to its potential to be highly efficient, especially at high salinity [7]. AGMD is different from other configurations because of the air gap between the membrane and the condensing surface, as shown in Fig.1. [9, 10]. The air gap imposes a high thermal resistance between the hot and the cold side to prevent heat loss and improve the energy efficiency, which is measured as the gained output ratio (GOR). However, the air gap also acts as a mass transfer resistance, decreasing the permeate flux condensed and collected on the condensing side. Because the system design goal is to generate more permeate flux without hampering the overall energy efficiency, the air gap thickness needs to be optimized [10, 11].

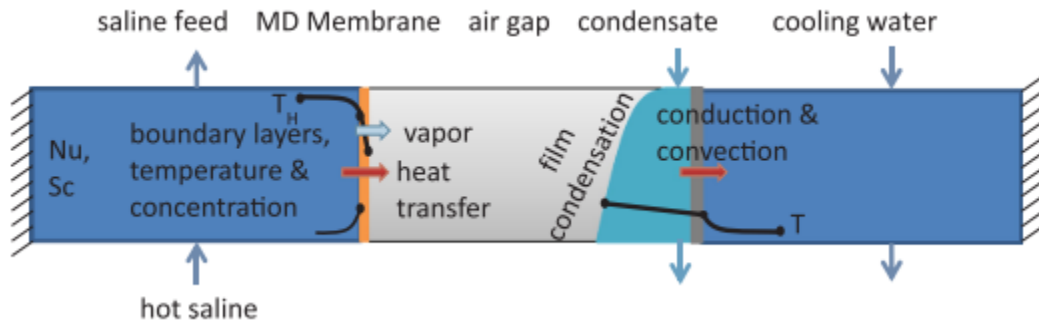


Fig.1 Schematic of air gap membrane distillation (AGMD) computational cell for numerical modeling that includes temperature variations in the concentration boundary layers, flow directions of vapor, heat, feed, cooling water and condensate [10]. Several hundred such cells are used to model a full membrane module.

Since the thermal resistance of conduction through air is very high, even small air gap thicknesses will prevent heat loss across the membrane. The mass transfer resistance is sensitive to the air gap thickness, and even small reductions the air gap lead to higher permeate flux generation. Given to this tradeoff, the optimal air gap size tends to be much smaller than those available previously. It can be seen in Fig.2(a) that decreasing air gap size to as small as 0.1 mm increases both GOR and the permeate flux. It is discussed in detail by Warsinger et.al. in their comprehensive study on condensation flow regimes [10]. The major obstacle in achieving air gap sizes below 3 mm is the risk of flooding the air gap with the permeate. This limitation coincides with the order of the capillary length scale of water, and is a function of the condensation regimes on the condensing plate and the rate at which water is removed out of the system [10].

In general, vapor condenses to form a laminar film on a condensing surface that thickens as condensate flows downward. If the air gap size is comparable to the film thickness, flooding will cause the AGMD

system to act like a permeate gap membrane distillation (PGMD) system. Flooding is to be avoided because water bridging of the air gap results in sharp decrease in thermal resistance, leading to loss of heat from the feed side to the permeate side.

To overcome the problem of air gap flooding, in recent years researchers have considered modifying the condensing surface to promote condensation regimes other than film-wise. Coating the condensing surface with hydrophobic coatings changes the regime to dropwise condensation, whereas superhydrophobic coatings having high contact angles and extremely low contact angle hysteresis can even lead to self-propelled jumping of condensate droplets from the surface. Faster droplet shedding at smaller droplet sizes, as characteristic of these condensing surfaces, has prevented flooding even at small air gap thickness of 0.2 mm. The GOR also increased by $2.1\times$ with more permeate flux generation [10].

In this work, we aim to experimentally evaluate such coatings and condensing surfaces that have the potential to form different kinds of condensation regimes on the surface. The inclination angle of the condensing surface can also be varied to observe the effect on the condensation regimes formed. The system shown in Fig.2(b) has a flexible membrane distillation module on which experiments can be conducted using different condensing surfaces. Variation in inclination angle while using smooth, flat condensing surface did not significantly improve the flux output and GOR. But will it affect the condensing regimes of nano-engineered surfaces differently is investigated in this work [10].

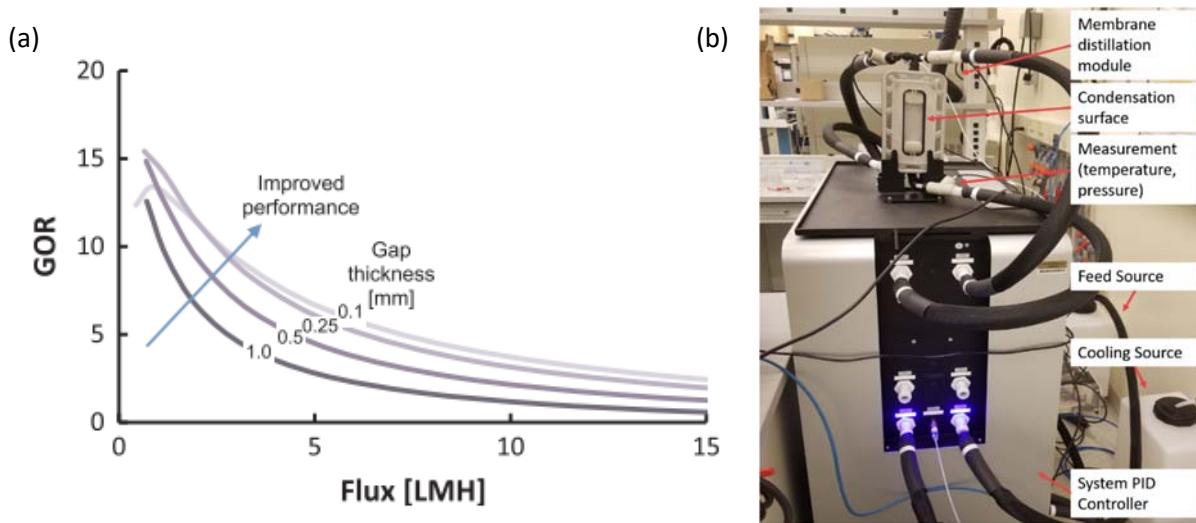


Fig.2 (a) Energy efficiency described by the Gained output ratio (GOR) versus permeate flux for varying air gap thickness [10]. It shows that the optimal gap thickness is below 0.25mm which is far less than the thickness possible with the current filmwise condensation regimes in AGMD. (b) Membrane distillation setup with flexibility to change air gap thickness, inclination angle and condensing surfaces.

2. CONDENSATION SURFACES AND FABRICATION TECHNIQUES

The engineered condensation surfaces investigated here are bioinspired, having nano and micro-scale textures of different morphologies and sizes that alter the surface adhesion and wetting characteristics [12]. In this work, these engineered surfaces are used as condensing surface in the MD setup. A description of selected engineered surfaces and their special characteristics are as follows:

1. Superhydrophobic surfaces with nanostructures provide high static contact angles ($\sim 165^\circ$) and very low hysteresis ($< 5^\circ$). During coalescence of droplets on such surfaces, the excess surface energy causes the coalesced droplet to jump off from the surface. The height and speed of droplet jumping from such superhydrophobic surfaces can be controlled by varying the size of the nanostructures [13] and their packing density [14]. It is critical to have control over the height of the jumping droplets, so as to prevent interaction with the membrane for differing air gap thicknesses, to ensure fast removal of condensate from the air gap. When the gap size is small, droplet interaction with membrane will introduce thermal connections across the membrane in addition to restricting droplet-shedding.
2. Another engineered surface is the shark-fin-like super-hydrophobic surface. The anisotropic nature of the surface can be controlled during fabrication to impart directional droplet jumping [15, 16]. Directional jumping of condensate droplets can be utilized to enhance droplet-shedding rate in MD system. It has also been found that the number of droplets jumping from such surfaces is less in total compared to superhydrophobic surfaces that do not affect the direction of jumping droplet, due to an increase in the horizontal velocity of the coalesced droplet [17]. Our work will help in comparing the rate of permeate removal from directional versus normal jumping droplet. Moreover, we also explore the effect of aligning the jumping direction with gravity in this study.
3. Patterned Biphilic Surfaces are surfaces with areas of super-hydrophobic and super-hydrophilic characteristics arranged in form of pattern around each other. Super-hydrophilic pathways for liquid flow on an otherwise superhydrophobic surface is an example of such surface. Such surface are explored to identify optimized pathway patterns for faster condensate removal [18].
4. Slippery liquid-infused porous surfaces (SLIPS) are hydrophobic surfaces featuring low contact angle hysteresis and higher droplet mobility compared to smooth hydrophobic surfaces due to the infused liquid present in the gaps of the surface nanostructures [19]. This infused liquid creates a liquid-liquid interface at the condensate droplet contact line which gives high droplet mobility, thus it will lead to easy and faster droplet shedding. The higher nucleation density on SLIPS support the same [20]. SLIPS are tested in MD setup over a period to observe if the properties degrade after repetitive use due to removal of the infused liquid [19]. The SEM images (Fig.3) of SLIPS and CuO nanowire based superhydrophobic surface (before coating) shows the difference in their nanostructure; which controls the type of condensation happening on the surface.
5. All the above engineered surfaces have issues with fabrication at scale, but superhydrophobic surfaces created using laser ablation show consistent surface wetting properties irrespective of the scale. Further, laser ablation is suitable for processing many metals to create desired surface morphologies. Lasers are accurate and programmable, allowing creation of intricate nanostructures further enhancing the super-hydrophobicity of a surface [21], [22]. We have tested the variation in hydrophobicity over time during continuous usage as condensation surface in MD setup, as degradation is common for many nanostructured superhydrophobic surfaces [23].

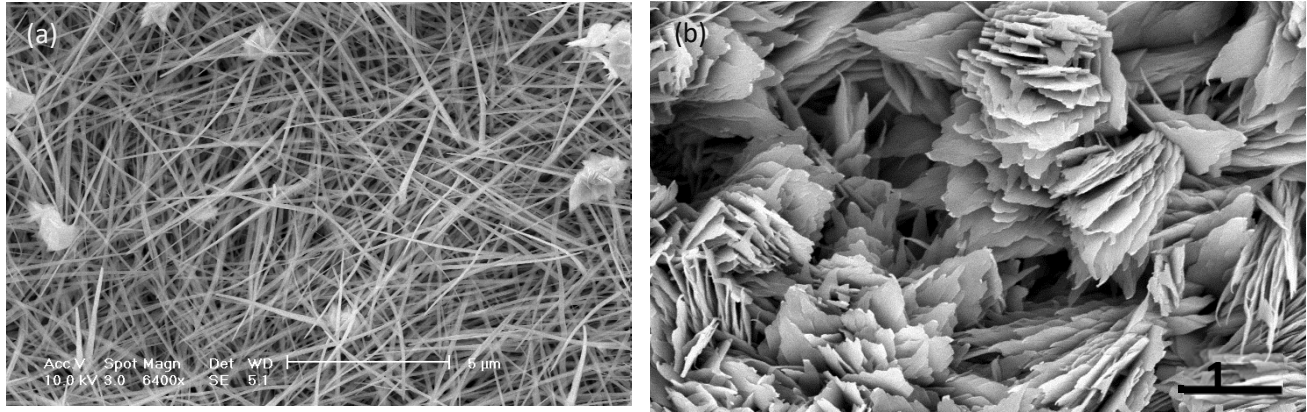


Fig 3. SEM images of (a) CuO nanowires grown on condensing surface before coating it with PDMS, the final step in making it superhydrophobic; scale bar = 5 μm (b) Slippery liquid infused porous surface (SLIPS); scale bar = 1 μm. The nano-structures on both the surfaces are different resulting in different surface characteristics.

Because the droplet shedding characteristics are inherently affected by the inclination angle of many superhydrophobic surfaces, all the above surfaces are also evaluated for a varying inclination angle within the MD setup [24]. We also test the effects of surface geometric features (macroscopic non-flatness) at millimeter scale on the condensing plate. It will vary the air gap thickness in certain regions of MD system affecting the mass transfer resistance. Varying mass transfer resistance in the MD system along the length will affect the condensation regime, Flux rate and GOR. [25]. Fig. 4 shows some types of possible condensation regimes during AGMD.

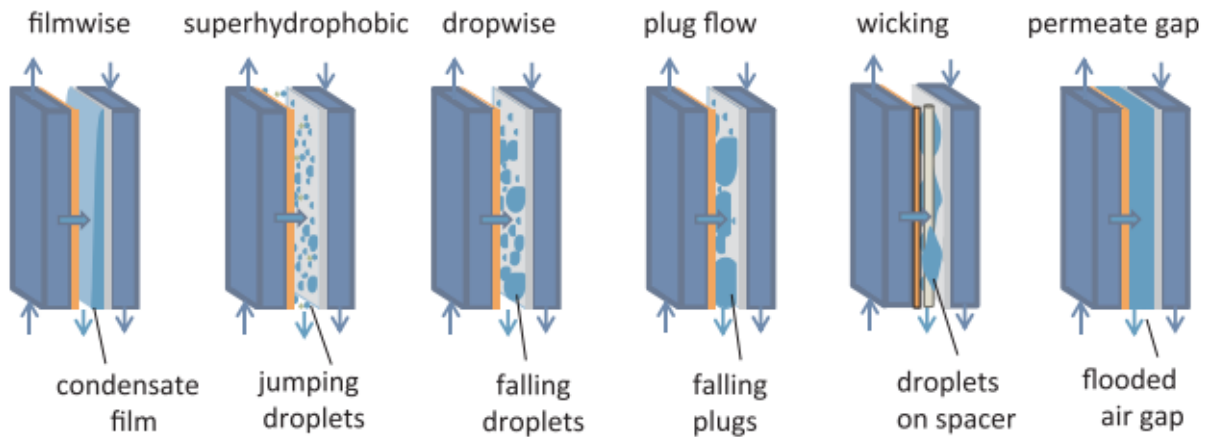


Fig.4 Examples of different condensation regimes possible during air gap membrane distillation (AGMD) [10]. The team members are the first to demonstrate jumping droplet and dropwise condensation.

3. CONCLUSION

We have fabricated and tested different types of condensing surfaces to observe the different condensation regimes that occur during air gap membrane distillation. The flexible test section of MD system allowed

for investigation of the effect of the inclination angle and size of the condensing surface on the condensation regimes. The permeate flux and energy efficiency associated with each condensation regime on the different condensing surfaces are compared.

4. ACKNOWLEDGEMENT

The authors would like to thank Jaichander Swaminathan from Indian Institute of Gandhinagar and John Lienhard V. from Department of Mechanical Engineering, Massachusetts Institute of Technology for their assistance in this work

REFERENCES

- [1] J. Swaminathan, H. W. Chung, D. M. Warsinger, and J. H. Lienhard V, "Simple method for balancing direct contact membrane distillation," *Desalination*, vol 383, pp. 53-59, 2016. <https://doi.org/10.1016/j.desal.2016.01.014>
- [2] E. Drioli, A. Ali, and F. Macedonio, "Membrane distillation: Recent developments and perspectives," *Desalination*, vol. 356, pp. 56–84, Jan. 2015. <https://doi.org/10.1016/j.desal.2014.10.028>
- [3] A. Servi, E. Guillen-Burrieza, D. M. Warsinger, W. Livernois, K. Notarangelo, J. Kharraz, J. H. Lienhard V, H. A. Arafat, K. K. Gleason, "The effects of iCVD film thickness and conformality on the permeability and wetting of MD membranes," *Journal of Membrane Science*, vol. 523, pp. 470–479, 2016.. <https://doi.org/10.1016/j.memsci.2016.10.008>
- [4] A. Luo and N. Lior, "Study of advancement to higher temperature membrane distillation," *Desalination*, vol. 419, pp. 88–100, Oct. 2017. <https://doi.org/10.1016/j.desal.2017.05.020>
- [5] D. M. Warsinger, A. Servi, G. B. Connors, M. O. Mavukkandy, H. A. Arafat, K. Gleason, and J. H. Lienhard, "Reversing membrane wetting in membrane distillation: comparing dryout to backwashing with pressurized air," *Environmental Science: Water Research & Technology*, vol. 3, pp. 930–939, 2017. <http://doi.org/10.1039/C7EW00085E>
- [6] R. Schwantes *et al.*, "Membrane distillation: Solar and waste heat driven demonstration plants for desalination," *Desalination*, vol. 323, pp. 93–106, Aug. 2013. <https://doi.org/10.1016/j.desal.2013.04.011>
- [7] G. W. Meindersma, C. M. Guijt, and A. B. De Haan, "Desalination and water recycling by air gap membrane distillation," *Desalination*, vol. 187, pp. 14–17, 2006.23 <https://doi.org/10.1016/j.desal.2005.04.088>
- [8] H. Geng, H. Wu, P. Li, and Q. He, "Study on a new air-gap membrane distillation module for desalination," *Desalination*, vol. 334, no. 1, pp. 29–38, Feb. 2014. <https://doi.org/10.1016/j.desal.2013.11.037>
- [9] L. Eykens, I. Hitsov, K. De Sitter, C. Dotremont, L. Pinoy, and B. Van der Bruggen, "Direct contact and air gap membrane distillation: Differences and similarities between lab and pilot scale," *Desalination*, vol. 422, pp. 91–100, Nov. 2017. <https://doi.org/10.1016/j.desal.2017.08.018>
- [10] D. M. Warsinger, J. Swaminathan, L. L. Morales, and J. H. Lienhard, "Comprehensive

- condensation flow regimes in air gap membrane distillation: Visualization and energy efficiency,” *Journal of membrane science* 555, 517-528, 2018. <https://doi.org/10.1016/j.memsci.2018.03.053>
- [11] A. S. Alsaadi *et al.*, “Modeling of air-gap membrane distillation process: A theoretical and experimental study,” *Journal of membrane science* 445: 53-65. 2013. <https://doi.org/10.1016/j.memsci.2013.05.049>
- [12] M. J. Hancock, K. Sekeroglu, and M. C. Demirel, “Bioinspired directional surfaces for adhesion, wetting, and transport,” *Adv. Funct. Mater.*, vol. 22, no. 11, pp. 2223–2234, 2012. <https://doi.org/10.1002/adfm.201103017>
- [13] X. Chen, J. A. Weibel, and S. V. Garimella, “Characterization of Coalescence-Induced Droplet Jumping Height on Hierarchical Superhydrophobic Surfaces,” *ACS Omega*, vol. 2, no. 6, pp. 2883–2890, Jun. 2017. <https://doi.org/10.1021/acsomega.7b00225>
- [14] M. D. Mulroe, B. R. Srijanto, S. F. Ahmadi, C. P. Collier, and J. B. Boreyko, “Tuning Superhydrophobic Nanostructures To Enhance Jumping-Droplet Condensation,” *ACS Nano*, vol. 11, no. 8, pp. 8499–8510, Aug. 2017. <https://doi.org/10.1021/acsnano.7b04481>
- [15] Q. An *et al.*, “Directional droplet-actuation and fluid-resistance reduction performance on the bio-inspired shark-fin-like superhydrophobic surface,” *J. Taiwan Inst. Chem. Eng.*, vol. 97, pp. 389–396, Apr. 2019. <https://doi.org/10.1016/j.jtice.2019.01.015>
- [16] J. Liu *et al.*, “Guided Self-Propelled Leaping of Droplets on a Micro-Anisotropic Superhydrophobic Surface,” *Angew. Chemie - Int. Ed.*, vol. 55, no. 13, pp. 4265–4269, 2016. <https://doi.org/10.1002/anie.201600224>
- [17] Z. Yuan, X. Wu, F. Chu, and R. Wu, “Numerical simulations of guided self-propelled jumping of droplets on a wettability gradient surface,” *Appl. Therm. Eng.*, vol. 156, pp. 524–530, Jun. 2019. <https://doi.org/10.1016/j.applthermaleng.2019.04.095>
- [18] X. Ji, D. Zhou, C. Dai, and J. Xu, “Dropwise condensation heat transfer on superhydrophilic-hydrophobic network hybrid surface,” *Int. J. Heat Mass Transf.*, vol. 132, pp. 52–67, Apr. 2019. <https://doi.org/10.1016/j.ijheatmasstransfer.2018.11.139>
- [19] S. Anand, A. T. Paxson, R. Dhiman, J. D. Smith, and K. K. Varanasi, “Enhanced Condensation on Lubricant-Impregnated Nanotextured Surfaces,” *ACS Nano*, vol. 6, no. 11, pp. 10122–10129, Nov. 2012. <https://doi.org/10.1021/nn303867y>
- [20] R. Xiao, N. Miljkovic, R. Enright, and E. N. Wang, “Immersion Condensation on Oil-Infused Heterogeneous Surfaces for Enhanced Heat Transfer,” *Sci. Rep.*, vol. 3, no. 1, p. 1988, Dec. 2013. <https://doi.org/10.1038/srep01988>
- [21] A. Y. Vorobyev and C. Guo, “Multifunctional surfaces produced by femtosecond laser pulses,” *J. Appl. Phys.*, vol. 117, p. 33103, 2015. <https://doi.org/10.1063/1.4905616>
- [22] A.-M. Kietzig, M. Negar Mirvakili, S. Kamal, P. Englezos, and S. G. Hatzikiriakos, “Laser-Patterned Super-Hydrophobic Pure Metallic Substrates: Cassie to Wenzel Wetting Transitions,” *J. Adhes. Sci. Technol.*, vol. 25, no. 20, pp. 2789–2809, 2011. <https://doi.org/10.1163/016942410X549988>
- [23] J. Xie, J. Xu, X. Li, and H. Liu, “Dropwise condensation on superhydrophobic nanostructure surface, Part I: Long-term operation and nanostructure failure,” *Int. J. Heat Mass Transf.*, vol. 129,

pp. 86–95, Feb. 2019. <https://doi.org/10.1016/j.ijheatmasstransfer.2018.09.100>

- [24] H. Wang, C. Liu, H. Zhan, and Y. Liu, “Droplet Asymmetric Bouncing on Inclined Superhydrophobic Surfaces,” *ACS omega*, vol. 4, no. 7, pp. 12238–12243, 2019. <http://dx.doi.org/10.1021/acsomega.9b01348>
- [25] Y. Zhao, D. J. Preston, Z. Lu, L. Zhang, J. Queeney, and E. N. Wang, “Effects of millimetric geometric features on dropwise condensation under different vapor conditions,” *Int. J. Heat Mass Transf.*, vol. 119, pp. 931–938, Apr. 2018. <https://doi.org/10.1016/j.ijheatmasstransfer.2017.11.139>